High-mobility group box-1 as an autocrine trophic factor in white matter stroke

Jun Young Choi (최준영)[a,b], Yuexian Cui (최월선)[a,c], Samma Tasneem Chowdhury[a,c], and Byung Gon Kim (김병곤)[a,b,c,1]

[a]Department of Brain Science, Ajou University School of Medicine, Suwon, 16499, Republic of Korea; [b]Department of Neurology, Ajou University School of Medicine, Suwon, 16499, Republic of Korea; and [c]Department of Biomedical Sciences, Neuroscience Graduate Program, Ajou University Graduate School of Medicine, Suwon, 16499, Republic of Korea

Edited by Gregg L. Semenza, The Johns Hopkins University School of Medicine, Baltimore, MD, and approved May 12, 2017 (received for review February 6, 2017)

Maintenance of white matter integrity in health and disease is critical for a variety of neural functions. Ischemic stroke in the white matter frequently results in degeneration of oligodendrocytes (OLs) and myelin. Previously, we found that toll-like receptor 2 (TLR2) expressed in OLs provides cell-autonomous protective effects on ischemic OL death and demyelination in white matter stroke. Here, we identified high-mobility group box-1 (HMGB1) as an endogenous TLR2 ligand that promotes survival of OLs under ischemic stress. HMGB1 rapidly accumulated in the culture medium of OLs exposed to oxygen–glucose deprivation (OGD). This conditioned medium exhibited a protective activity against ischemic OL death that was completely abolished by immunodepletion of HMGB1. Knockdown of HMGB1 or application of glycyrrhizin, a specific HMGB1 inhibitor, aggravated OGD-induced OL death, and recombinant HMGB1 application reduced the extent of OL death in a TLR2-dependent manner. We confirmed that cytosolic translocation of HMGB1 and activation of TLR2-mediated signaling pathways occurred in a focal white matter stroke model induced by endothelin-1 injection. Animals with glycyrrhizin coinjection showed an expansion of the demyelinating lesion in a TLR2-dependent manner, accompanied by aggravation of sensorimotor behavioral deficits. These results indicate that HMGB1/TLR2 activates an autocrine trophic signaling pathways in OLs and myelin to maintain structural and functional integrity of the white matter under ischemic conditions.

white matter stroke | oligodendrocyte | toll-like receptor 2 | HMGB1 | myelination

White matter in the vertebrate brain is characterized by the presence of myelinated axonal fibers and glial cells, predominantly myelin-producing oligodendrocytes (OLs) (1). The myelin sheath enables rapid communication of neural signals at a millisecond timescale between different parts of the cerebral cortex or different regions of the CNS (2). Therefore, maintaining the integrity of white matter in health and disease, especially of OLs and the myelin sheath, is critical to the performance of a variety of brain functions. Furthermore, recent studies have shown that myelination and OL generation in adulthood are actively regulated in response to neural activities (3, 4), highlighting the potential contribution of white matter plasticity to learning and higher cognitive functions.

Ischemic stroke that occurs in the white matter often results in degeneration of OLs and demyelination (5, 6). Consequently, patients with white matter stroke suffer from a wide range of neurological dysfunctions. For example, focal ischemic stroke in the internal capsule may result in severe hemiparesis (7). Furthermore, both cognitive deficits and gait disturbance are hallmarks of Binswanger's subcortical vascular dementia that is the most severe form of white matter stroke (8). How ischemia leads to OL degeneration and demyelination is poorly understood. We previously reported that toll-like receptor 2 (TLR2) expressed in OLs plays a protective role in ischemic demyelination and OL death (9). The purpose of the present study was to identify an endogenous ligand that stimulates TLR2 to support OL survival. Here, we provide evidence that high-mobility group box-1 (HMGB1) derived from damaged OLs supports survival of neighboring OLs in a TLR2-dependent manner. We also report that inhibition of HMGB1 leads to aggravation of ischemic demyelination and exacerbation of neurologic dysfunction in an animal model of white matter stroke, suggesting a hitherto uncharacterized function of HMGB1 as an autocrine trophic factor to maintain the structural and functional integrity of the white matter under ischemic conditions.

Results

HMGB1 Is Released from OLs Damaged by Oxygen–Glucose Deprivation. Our previous study showed that deletion of TLR2 worsened death of purified OLs in culture after oxygen–glucose deprivation (OGD), an in vitro ischemic insult (9). We speculated that an endogenous ligand for TLR2 was present in the culture and activated TLR2-mediated protective signaling in OLs. Because the OLs were in dissociated cultures, any potential endogenous ligand would have to be released from OLs in response to OGD insult. Therefore, we screened the conditioned medium (CM) from cultured OLs after OGD exposure for the presence of soluble known TLR2 ligands, including heat shock protein family members and HMGB1 (10–13). Western blot experiments revealed the presence of HMGB1, but not heat shock protein 90, 70, or 60, in the CM collected 6 h after the 2-h OGD treatment (Fig. 1*A*). HMGB1 was detected as early as 30 min after the outset of OGD, rapidly accumulated between 30 and 60 min, and reached a plateau by 90 min (Fig. 1*B*). Immunofluorescence staining confirmed expression of HMGB1 in cultured OLs (Fig. 1*C*) and in OLs in the internal capsule in the brain as well (Fig. 1*D*), indicating that OLs are the likely source of HMGB1 in the CM and could produce it in vivo.

Significance

Ischemic stroke in white matter induces degeneration of oligodendrocytes (OLs) and myelin. How ischemia leads to white matter degeneration remains elusive, and there is therefore no specific treatment to prevent ischemic white matter damage. Here we provide evidence that HMGB1 released from ischemic OLs may provide TLR2-dependent autocrine trophic effects on neighboring OLs. Injection of an HMGB1 inhibitor exacerbated the structural and functional outcomes in a focal white matter stroke model, suggesting a function for HMGB1 as an endogenous trophic factor for OLs and myelin sheath under ischemia. Thus, our study identified HMGB1 as a stress-induced signal that maintains structural and functional integrity of the white matter and provides a target for therapeutic development in white matter stroke.

Author contributions: J.Y.C. and B.G.K. designed research; J.Y.C., Y.C., and S.T.C. performed research; J.Y.C., Y.C., S.T.C., and B.G.K. analyzed data; and J.Y.C. and B.G.K. wrote the paper.

The authors declare no conflict of interest.

This article is a PNAS Direct Submission.

[1]To whom correspondence should be addressed. Email: kimbg@ajou.ac.kr.

This article contains supporting information online at www.pnas.org/lookup/suppl/doi:10.1073/pnas.1702035114/-/DCSupplemental.

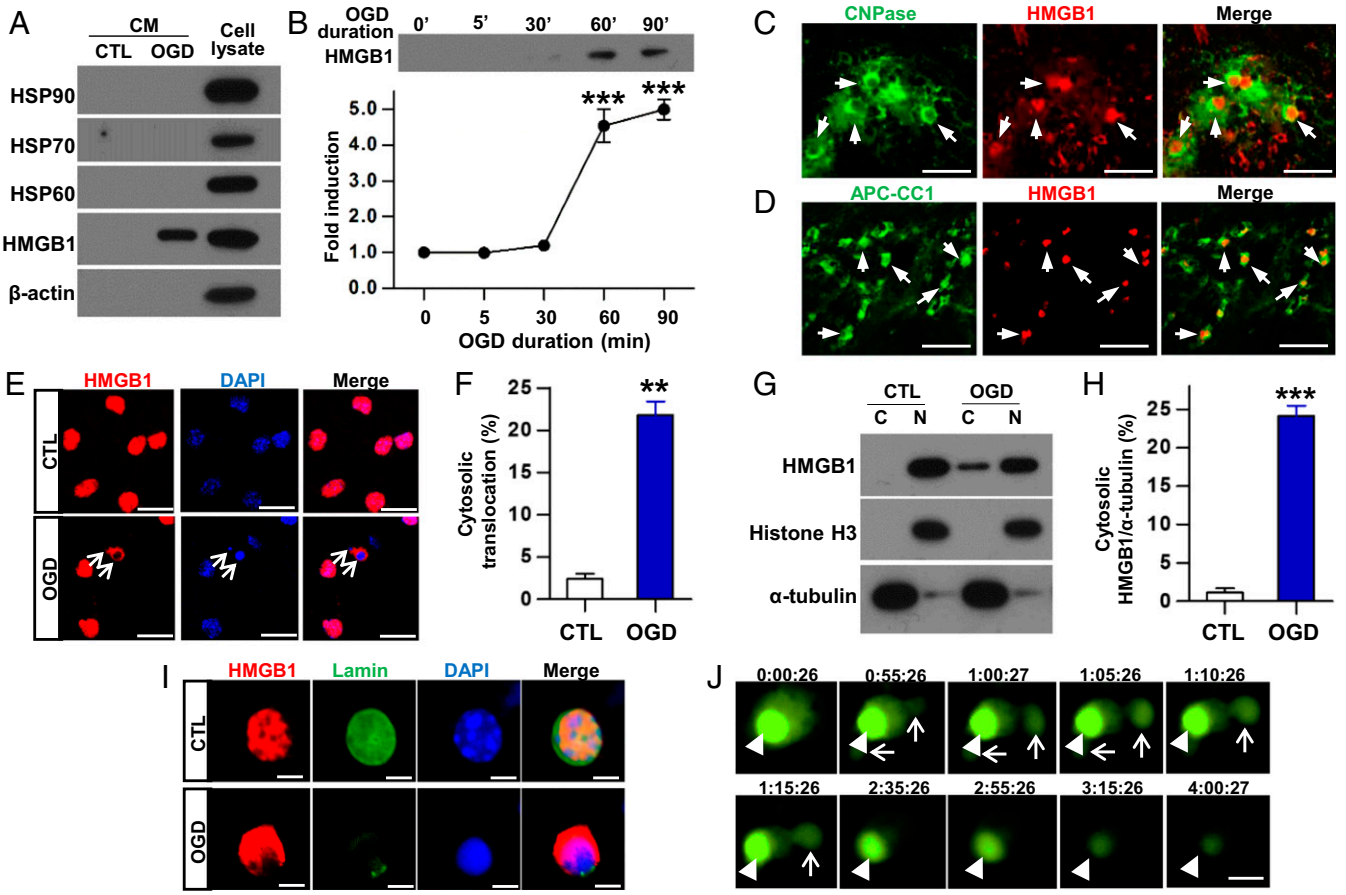

Fig. 1. Accumulation of HMGB1 in oligodendrocyte culture medium and translocation after oxygen–glucose deprivation (OGD). (*A*) Representative immunoblots probed for heat shock protein family members and HMGB1 protein. Conditioned medium (CM) was collected from primary oligodendrocyte (OL) cultures 6 h after a 2-h OGD period. Control (CTL) CM was collected without OGD. Brain lysate was used as a positive control. (*B*) Representative immunoblot to illustrate the time course of HMGB1 accumulation. CM was collected at the designated time points after the outset of OGD treatment. Quantification graph showing the level of HMGB1 at different time points after the beginning of OGD. ***$P < 0.001$ compared with the condition without OGD (0′) by one-way ANOVA followed by Tukey's post hoc analysis. $n = 3$ for each time point. (*C*) Expression of HMGB1 in cultured OLs. OLs were identified by 2′,3′-cyclic-nucleotide 3′-phosphodiesterase (CNPase) immunoreactivity. (Scale bars, 50 μm.) (*D*) Expression of HMGB1 in mature OLs in the internal capsule of the brain. Mature OLs were identified by APC-CC1 immunoreactivity. (Scale bars, 100 μm.) (*E*) Representative images of cultured OLs with OGD or CTL condition (without OGD) immunostained using anti-HMGB1 antibodies. Nuclear chromatin material was visualized by DAPI staining. Cultured OLs were fixed 10 min after completion of the 2-h OGD. Arrows indicate the OLs with nuclear condensation and cytosolic translocation of HMGB1. (Scale bars, 20 μm.) (*F*) Quantification graph of the percentage of OLs with cytosolic localization of HMGB1. **$P < 0.01$ compared with CTL by Student's *t* test. More than 800 OLs were examined for each independent culture and three independent cultures for each group were used for statistical analysis ($n = 3$). (*G*) Representative immunoblots showing cytosolic location of HMGB1 immediately after 2-h OGD. C, cytosolic fraction; N, nuclear fraction. (*H*) Quantification graph of relative HMGB1 ratio to cytosolic α-tubulin. ***$P < 0.001$ compared with CTL. $n = 3$ independent cultures. (*I*) Representative highly magnified images of individual OLs in CTL or OGD-treated cultures. The nuclear membrane was visualized by using antibodies directed against lamin. Nuclear chromatin material was visualized by DAPI staining. (Scale bars, 5 μm.) (*J*) Time-lapse fluorescence images of a cultured OL transfected with the HMGB1–GFP plasmid. To mimic OGD insult, $CoCl_2$-containing glucose-free medium was used. The number above each image indicates the image-capture time. Arrowheads indicate HMGB1–GFP signals in the nucleus. Arrows indicate HMGB1–GFP signals released into the extracellular space. (Scale bar, 10 μm.)

A previous study reported that HMGB1 translocates from the nucleus to the cytosol after ischemic insult (14). Consistent with this study, we observed extranuclear translocation of HMGB1 after OGD insult in cultured OLs (Fig. 1*E*). In the control condition without OGD, extranuclear localization of HMGB1 was rarely detected. However, more than 20% of cultured OLs exhibited cytosolic localization of HMGB1 after OGD (Fig. 1 *E* and *F*). In the majority of the cells showing extranuclear translocation of HMGB1, the DAPI signal was condensed, indicating that the cells were damaged. HMGB1 translocation to cytosolic compartment was also confirmed by a biochemical fractionation. OL lysates were fractionated into cytosolic and nuclear fractions, and immunoblotting with HMGB1 antibody showed cytosolic immunoreactivity in OLs with OGD but not OLs without OGD (Fig. 1*G*). Relative immunoreactivity of HMGB1 to α-tubulin showed a significant increase in the cytosolic compartment in OLs with OGD (Fig. 1*H*). In higher magnification images, HMGB1 was found exclusively in the area enclosed by the nuclear membrane in OLs without OGD (Fig. 1*I*). In cells showing nuclear condensation following OGD, HMGB1 was located in the cytosolic space near the area of nuclear membrane disruption. To obtain convincing evidence of HMGB1 release from dying OLs under ischemic stress, we performed time-lapse live imaging of cultured OLs transfected with an HMGB1–GFP plasmid. HMGB1 release was observed after $CoCl_2$ application, which induces hypoxia. The GFP signal accumulated transiently in the vicinity of transfected OLs (Fig. 1*J* and Movie S1), whereas there was no evidence of extracellular GFP signal in OLs without ischemic stress (Movie S2). The intensity of extracellular HMGB1–GFP signal accumulation decreased as nuclear HMGB1–GFP signals gradually disappeared over the course of the ∼4 h of $CoCl_2$ exposure.

HMGB1 Provides Protective Effects on Cultured OLs Under OGD Insult. To determine whether the HMGB1 released into the CM is protective to cultured OLs, CM obtained from cultured OLs exposed to OGD was applied to a separate batch of cultured OLs. CM treatment significantly reduced OGD-induced OL death (Fig. 2*A*). When HMGB1 in the CM was depleted by immunoprecipitation using HMGB1 antibodies (Fig. S1), this HMGB1-depleted CM (ΔCM) completely lacked the protective activity (Fig. 2*A*). The OL-protective effects of CM were not observed when the CM was applied to TLR2 (−/−) OLs, and the extent of cell death was not affected by ΔCM treatment in TLR2 (−/−) OLs (Fig. 2*B*). We tested whether application of glycyrrhizin, a molecule that binds HMGB1 and can block its activity (15), would raise OGD-induced OL death rate. Application of glycyrrhizin to control cultures without OGD had no effect, but aggravated OGD-induced OL death in a dose-dependent manner (Fig. 2*C*). We next determined whether HMGB1 knockdown could aggravate OGD-induced OL death. In OL cultures transfected with HMGB1 siRNA, HMGB1 protein levels in OL lysates and CM were lowered effectively (Fig. S2), and the rate of OGD-induced OL death substantially increased (Fig. 2*D*). Addition of glycyrrhizin did not influence the extent of OL death by siRNA treatment. These results indicate that HMGB1 released from OLs in response to OGD plays an essential role in an endogenous mechanism that is protective against ischemic OL death in vitro. We next confirmed the protective effects of exogenously applied HMGB1 on OGD-induced OL death. Recombinant HMGB1 was applied to OLs after OGD. HMGB1 at 0.1 or 1.0 ng/mL significantly reduced the extent of OL death (Fig. 2*E*). Application of HMGB1 at these concentrations failed to reduce the death rate of TLR2 (−/−) OLs (Fig. 2*F*), confirming that the protective effects of HMGB1 are dependent on TLR2. Treatment of glycyrrhizin to the OGD-exposed OLs effectively blocked the prosurvival effects of exogenous HMGB1 at concentrations similar to those that were effective for endogenous HMGB1 (Fig. 2*E*).

To determine the intracellular signaling pathways involved in the HMGB1/TLR2-mediated protective effects on OLs, we examined the levels of IκB-α, phospho-ERK1/2, and phospho-CREB, which are known signaling molecules downstream of TLR2 (16). OGD insult resulted in a decrease in the level of IκB-α 15 min after the 2-h OGD treatment, with recovery occurring by 60 min (Fig. S3*A*). Glycyrrhizin treatment prevented the decrease of IκB-α, whereas HMGB1 treatment tended to augment the early reduction of IκB-α (Fig. S3*B*). Levels of both phospho-ERK1/2 and phospho-CREB changed similarly. Phosphorylation of both ERK1/2 and CREB increased markedly after OGD: There was an approximate threefold increase at 15 min (Fig. S3 *A*, *C*, and *D*). Inhibition of HMGB1 by applying glycyrrhizin substantially prevented the OGD-induced phosphorylation of ERK1/2 and CREB. In contrast, HMGB1 treatment significantly enhanced the OGD-induced

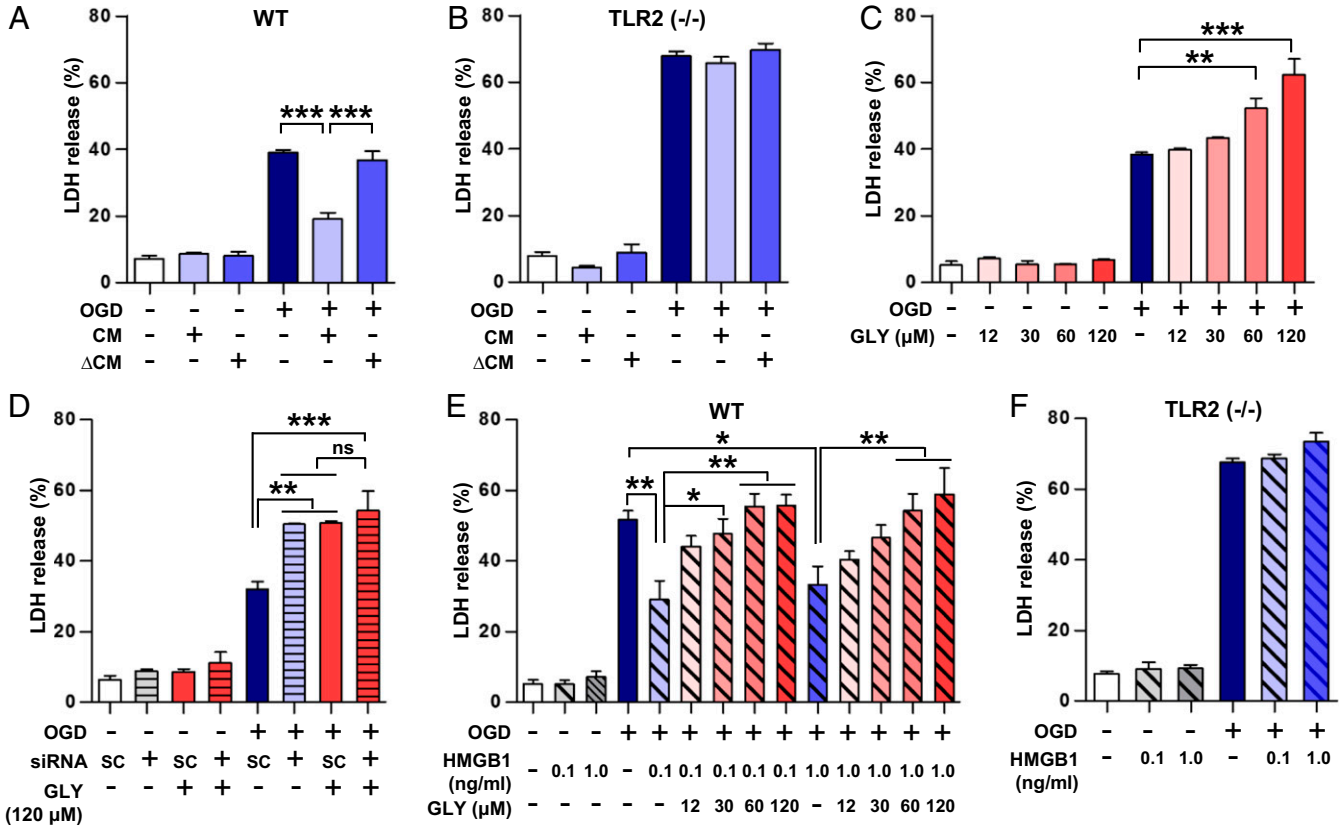

Fig. 2. HMGB1 promotes survival of cultured oligodendrocytes after oxygen–glucose deprivation. (*A* and *B*) Quantification graph of LDH assays in cultured oligodendrocytes (OLs) from wild-type (*A*) or TLR2 (−/−) (*B*) mice. When indicated, the culture medium was replaced after the 2-h OGD treatment period with conditioned medium (CM) collected from cultured OLs 6 h after completing OGD or CM collected in the same manner from which HMGB1 was immunodepleted (ΔCM). $n = 3$ independent cultures for both experiments. (*C* and *D*) Quantification graphs of LDH assays to examine effects of glycyrrhizin (GLY) treatment (*C*) or siRNA-mediated HMGB1 knockdown (*D*) and on OL death after OGD. GLY at a 120-μL concentration was also treated in conditions as indicated. Sc, scrambled control nontargeting siRNA. $n = 3$ independent cultures for both experiments. (*E* and *F*) Quantification graphs of LDH assays to examine the effects of applying recombinant HMGB1 on cell death of wild-type (*E*) and TLR2 (−/−) (*F*) OLs. Escalating doses of GLY were treated in conditions as indicated. $n = 3$ or 4 independent cultures for wild-type OLs. Ns, not significant. $n = 3$ independent cultures for TLR2 (−/−) OLs. $^*P < 0.05$, $^{**}P < 0.01$, and $^{***}P < 0.001$ by one-way ANOVA followed by Tukey's post hoc analysis.

activation of both signaling molecules and prolonged their activation to at least 60 min (Fig. S3 *A*, *C*, and *D*).

Endothelin-1 Injection Induces Cytosolic Translocation of HMGB1 in Vivo and Activates Its Downstream Signaling Pathways. Our previous study showed that TLR2 provides endogenous protection against ischemic demyelination induced by endothelin-1 (ET-1) injection (9). We therefore examined whether cytosolic translocation of HMGB1 occurs in the same model. HMGB1 was detected exclusively in the nuclear fraction of lysates of the internal capsule from the hemisphere contralateral to the injection (Fig. 3*A*). In contrast, overt HMGB1 immunoreactivity was found in the cytosolic fraction of the internal capsule from the ipsilateral side. The intensity of cytosolic HMGB1 signal relative to that of α-tubulin was markedly increased in the ipsilateral side (Fig. 3*B*). Furthermore, ET-1 injection induced phosphorylation of ERK1/2 and CREB (Fig. 3 *C*–*E*), both of which were activated by HMGB1 treatment in cultured OLs (Fig. S3). This in vivo activation of the two signaling pathways was almost completely prevented by coinjection of glycyrrhizin and did not occur in TLR2 (–/–) animals (Fig. 3 *C*–*E*). We also determined whether the activation of the signaling proteins after ET-1 injection occurred in the cells with OL lineage. Approximately 12% of Olig2$^+$ cells in the internal capsule in the vicinity of the ET-1 injection core colocalized with phospho-CREB immunoreactivity in wild-type animals (Fig. 3 *F* and *G*). The colocalization of OL lineage cells with phospho-CREB was virtually absent when ET-1 was coinjected with glycyrrhizin or injected into TLR2 (–/–) animals (Fig. 3 *F* and *G*).

Glycyrrhizin Aggravates ET-1–Induced Demyelinating Pathology and Behavioral Deficits. We hypothesized that inhibition of HMGB1 in the ET-1 white matter stroke model would attenuate an endogenous protective mechanism and therefore result in an expansion of the demyelinating pathology. Glycyrrhizin (240 μM) or PBS was coinjected with ET-1 into the internal capsule, and the volume of the demyelinating lesion was compared 7 d after injection. The average size of the demyelinating lesion after glycyrrhizin coinjection was approximately twice that in the PBS coinjection group (Fig. 4 *A* and *C*). As expected, ET-1 injection (with PBS) in TLR2 (–/–) mice resulted in an expansion of the demyelinating lesion compared with that in wild-type animals (Fig. 4 *B* and *C*). Furthermore, coinjection of glycyrrhizin failed to aggravate ET-1–induced demyelinating pathology in TLR2 (–/–) mice, indicating that HMGB1 signaling in vivo is transmitted through TLR2.

Finally, we determined whether expansion of the ischemic demyelinating lesion affected neurobehavioral outcomes by performing the corner test and the pole test. Both tests are frequently used in ischemic injury models: The corner test is used to assess

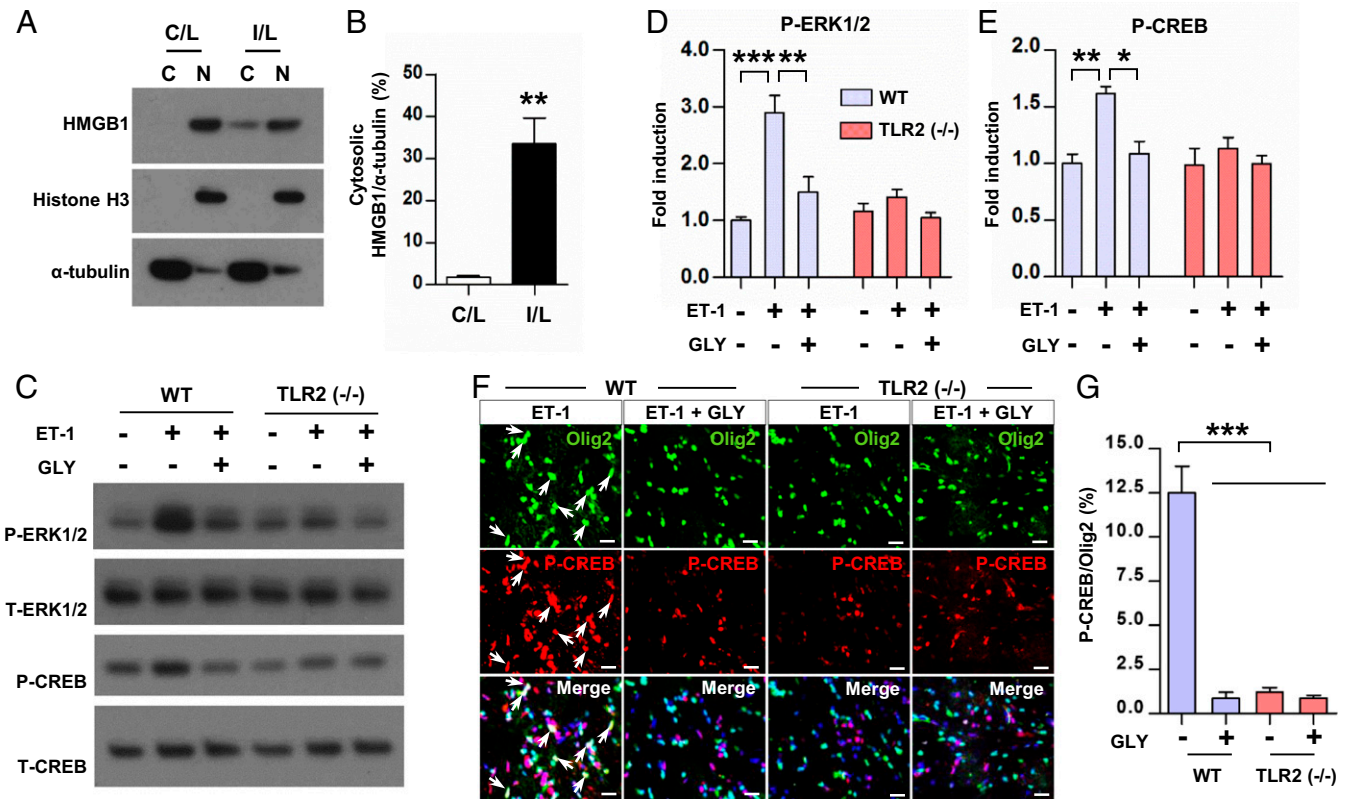

Fig. 3. Endothelin-1 (ET-1) injection induces cytosolic translocation of HMGB1 and activates its downstream signaling pathways. (*A*) Representative blots illustrating cytosolic translocation of HMGB1 after ET-1 injection. Lysates from the internal capsules ipsilateral (*I*/L) and contralateral (*C*/L) to the lesion site were obtained 3 h after injection and separated into cytosolic (C) and nuclear (N) fractions. Immunoreactivity for nuclear protein histone H3 was used to verify the fractionation. (*B*) Quantification graph of the cytosolic HMBG1 immunoreactivity (expressed as a percentage of the intensity of α-tubulin immunoreactive bands) in the ipsilateral and contralateral internal capsules. $^{**}P < 0.01$ by Student's *t* test. $n = 4$ animals for each group. (*C*) Representative blots examining phosphorylation of ERK1/2 and CREB in the internal capsule lysates obtained 24 h after ET-1 injection in wild-type and TLR2 (–/–) mice. When indicated, glycyrrhizin (GLY) was coinjected with ET-1. (*D* and *E*) Quantification graphs of the levels of phosphorylated ERK1/2 (*D*) and CREB (*E*) in ipsilateral internal capsule lysates. $^{*}P < 0.05$, $^{**}P < 0.01$, and $^{***}P < 0.001$ by one-way ANOVA followed by Tukey's post hoc analysis. $n = 3$ animals for each group. (*F*) Immunohistochemical detection of phosphorylated CREB (red) in oligodendrocytes (OLs). OLs were identified by olig2 immunoreactivity (green). (Scale bars, 20 μm.) (*G*) Quantification graph of the percentage of Olig2$^+$ cells colocalized with phosphor-CREB immunoreactivity. $^{***}P < 0.001$ by one-way ANOVA followed by Tukey's post hoc analysis. $n = 7, 7, 7,$ and 8 animals for WT animals without or with GLY, and TLR2 (–/–) animals without or with GLY, respectively.

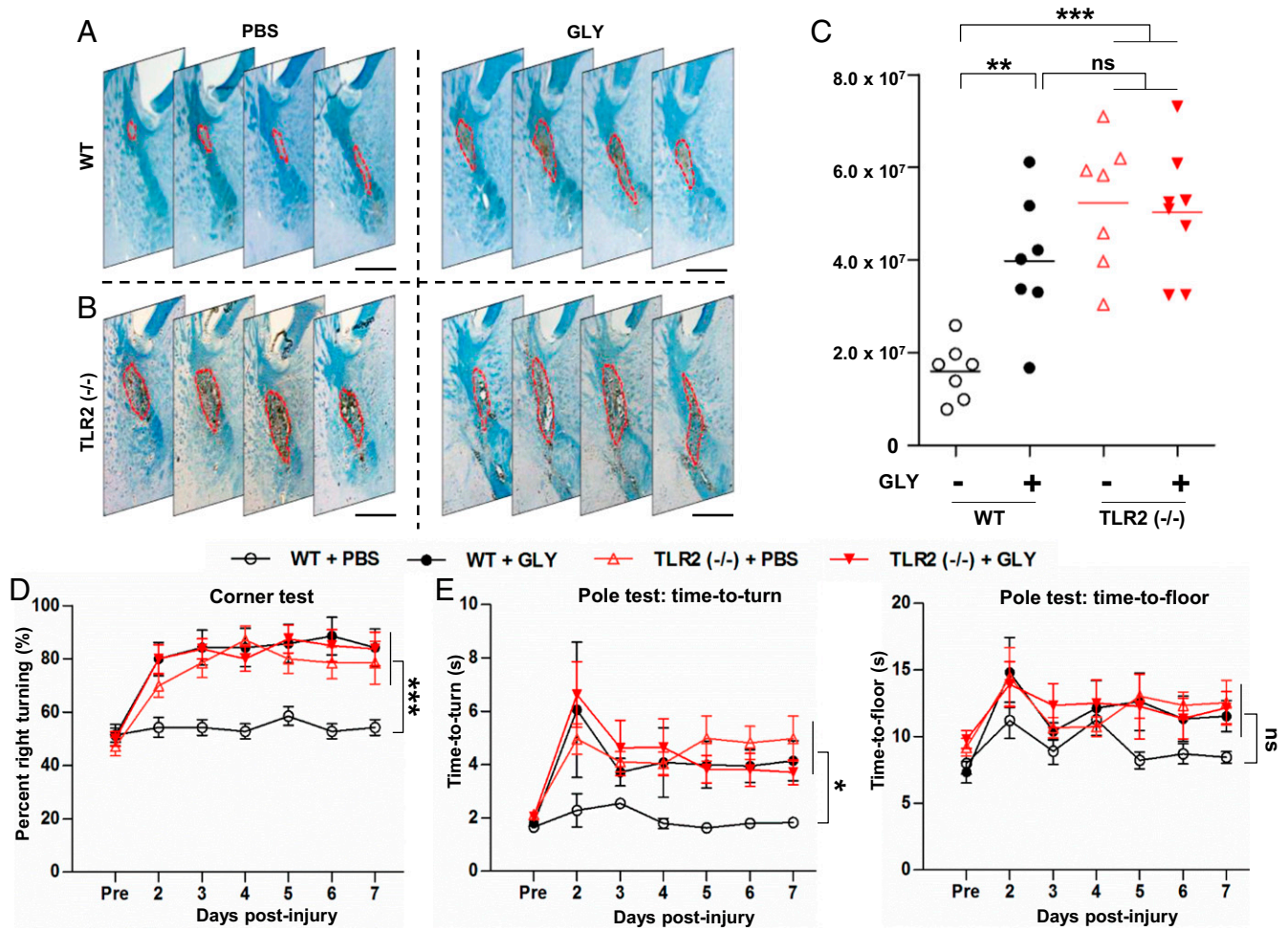

Fig. 4. Glycyrrhizin coinjection enlarges the endothelin-1–induced demyelinating lesion and aggravates behavioral deficits. (*A* and *B*) Representative images of serial coronal sections stained with eriochrome cyanine from (*A*) WT or (*B*) TLR2 (−/−) animals. Animals in both groups were injected with ET-1 together with PBS or glycyrrhizin (GLY). The brains were fixed at 7 d postinjection. The intersection distance is 80 μm. Red lines represent lesion borders. (Scale bars, 500 μm.) (*C*) Quantification graph of the demyelinating lesion volume measured by Neurolucida 3D reconstruction. $n = 7$, 7, 7, and 8 animals for WT with PBS, WT with GLY, TLR2 (−/−) with PBS, and TLR2 (−/−) with GLY, respectively. $^{**}P < 0.01$ and $^{***}P < 0.001$ by one-way ANOVA followed by Tukey's post hoc analysis. Ns, not significant. (*D*) Quantification graph of the corner test results performed before ET-1 injection and everyday after the injection for 7 d. Four groups of animals were evaluated: WT animals with coinjection of PBS ($n = 7$), WT animals with coinjection of GLY, TLR2 (−/−) animals with coinjection of PBS ($n = 7$), and TLR2 (−/−) animals with coinjection of GLY ($n = 8$). (*E*) Quantification graphs of the pole test results measuring the latency to downward turning of the head (time to turn) and the latency to reach the floor (time to floor) performed on the same days as for the corner test. $^{*}P < 0.05$ and $^{***}P < 0.001$ by repeated measures two-way ANOVA followed by Bonferroni's post hoc analysis. Ns, not significant.

sensory and motor asymmetries (17–19), whereas the pole test is used to examine motor dysfunction (19, 20). In the corner test, ET-1 injection with PBS to the right internal capsule resulted in a slight preference to turn right (Fig. 4*D*). Wild-type mice with glycyrrhizin coinjection showed a marked right turn preference from 1 to 7 d postinjection, the last day of the test. Right turn preference was also observed in TLR2 (−/−) mice following ET-1 injection alone (Fig. 4*D*). Glycyrrhizin coinjection did not aggravate this behavioral outcome in TLR2 (−/−) mice. In the pole test, two parameters were measured: the time taken to turn the head downward (time to turn) and the time taken to descend the pole and reach the floor (time to floor). In wild-type animals, glycyrrhizin coinjection markedly prolonged time to turn, but time to floor was not significantly affected (Fig. 4*E*). Time to turn was significantly increased in TLR2 (−/−) animals compared with wild-type animals when ET-1 alone was injected, and glycyrrhizin injection did not affect time to turn in TLR2 (−/−) mice. Time to floor was not significantly influenced by genotype. The values of the right turning preference in the corner test and the time to turn in the pole test were significantly correlated with the volumes of the ischemic demyelinating lesion (Fig. S4), suggesting that the extent of the ischemic demyelination is a meaning determinant of behavioral deficit in this model of white matter stroke.

HMGB1 Does Not Induce Proinflammatory Activation of Microglial Cells. Extracellularly released HMGB1 can activate microglial cells thereby promoting neuroinflammation (21, 22). It is possible that HMGB1 released from OLs after ET-1 injection could affect postischemic proinflammatory reactions mediated by microglial cells. However, there was no difference in the intensity of Iba-1 immunoreactivity within the ischemic demyelinating lesions between the groups with coinjection of PBS and glycyrrhizin (Fig. 5 *A* and *B*), indicating that HMGB1 did not influence the extent of microglial activation. To further investigate the potential influence of HMGB1 on phenotypic changes in microglial cells, cultured microglial cells were treated with recombinant HMGB1 and the collected microglia conditioned medium (MCM) was applied to cultured OLs exposed to OGD. The extent of OL death in cultures

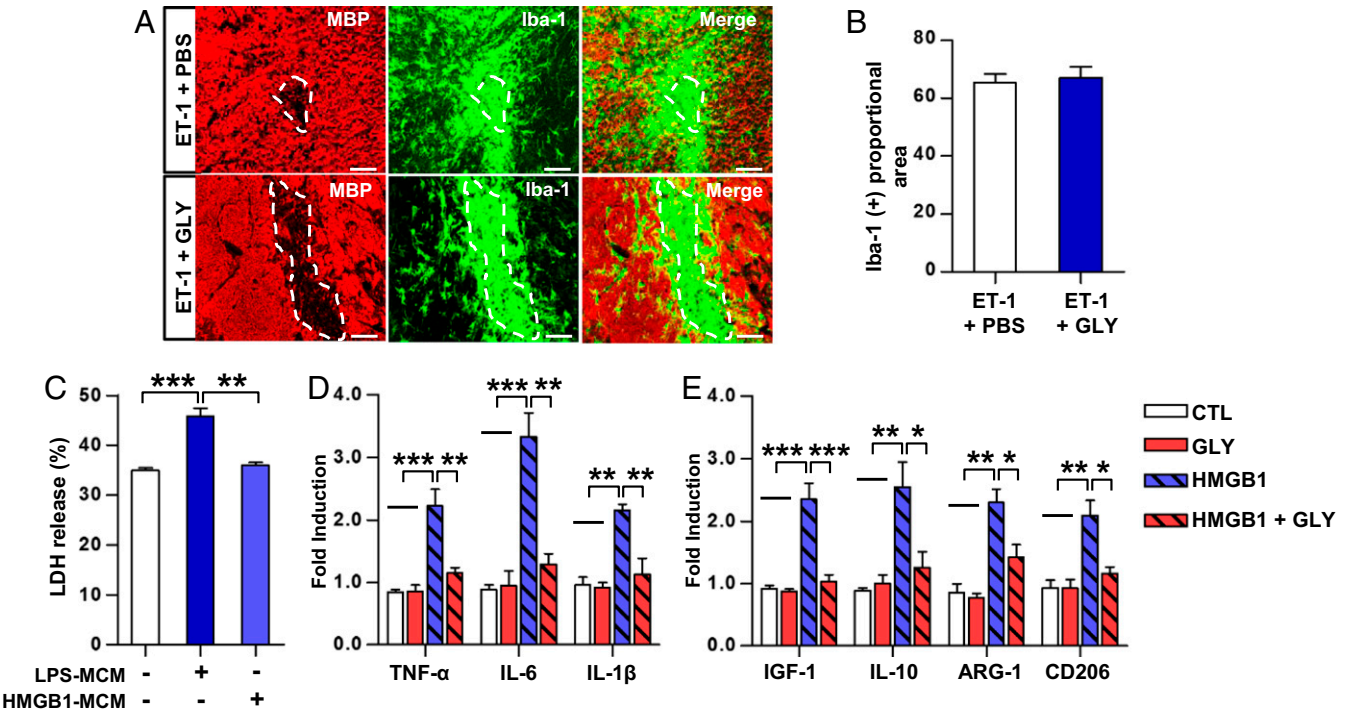

Fig. 5. HMGB1 does not induce proinflammatory activation of microglial cells. (*A*) Representative images of coronal brain sections containing the internal capsule obtained from animals injected with endothelin-1 (ET-1) and PBS or glycyrrhizin (GLY). The brain sections were stained with antibodies against myelin basic protein (MBP) (red) and Iba-1 (green). Dotted lines indicate the borders of demyelinating lesions. (Scale bars, 50 μm.) (*B*) Quantification graph of the proportion of the MBP^- lesion area that was Iba-1^+ (bordered by the dotted lines). (*C*) Quantification graph of LDH assays to examine effects of microglia conditioned media (MCM) on OL death after oxygen–glucose deprivation. MCM was collected from primary microglial cultures for 72 h after the 3-h incubation with LPS (100 ng/mL) or HMGB1 (1 ng/mL). (*D* and *E*) Quantification graphs of mRNA levels for genes related to either M1 (*D*) or M2 (*E*) polarization of microglial cells. Primary cultured microglial cells were incubated with control (CTL) PBS, GLY (120 μL) alone, recombinant HMGB1 (1.0 ng/mL) alone, or a combination of both HMGB1 and GLY for 3 h and then harvested for mRNA extraction. $n = 3$ and 4 independent cultures for measurement of M1- and M2-related genes, respectively. $^*P < 0.05$, $^{**}P < 0.01$, and $^{***}P < 0.001$ by one-way ANOVA followed by Tukey's post hoc analysis.

with HMGB1-treated MCM was not significantly different from that under control conditions (OGD alone without any treatment), whereas the treatment with lipopolysaccharides (LPS)-treated MCM used as a positive control resulted in an aggravation of OL death (Fig. 5*C*). HMGB1 treatment of microglial cells significantly up-regulated expression of a panel of proinflammatory genes such as TNF-α, IL-6, and IL-1β, all of which have been linked to induction of OL death (23–25) (Fig. 5*D*). HMGB1 simultaneously increased expression of IGF1, which is known to provide trophic effects on OLs (26) (Fig. 5*E*). Moreover, expression of the antiinflammatory marker gene IL-10 was also substantially up-regulated by HMGB1 treatment. HMGB1 also significantly up-regulated the expression of M2 marker genes such as Arginase-1 and CD206. Addition of glycyrrhizin effectively blocked the HMGB1-induced up-regulation of all of the above genes, whereas glycyrrhizin alone did not influence gene expression levels (Fig. 5 *D* and *E*). Collectively, these data suggest that HMGB1 does not skew the functional phenotype of microglial cells toward one that is cytotoxic to OLs because the expression of both M1 and M2 marker genes is simultaneously up-regulated by HMGB1.

Discussion

Our study demonstrated that damaged OLs exposed to ischemic conditions in culture release HMGB1 and that the released HMGB1 exerts protective effects on neighboring OLs in a TLR2-dependent manner. We also found in vivo evidence of HMGB1 translocation with activation of TLR2-dependent signaling pathways in a focal white matter stroke model induced by ET-1 injection. Inhibition of HMGB1 by glycyrrhizin resulted in an expansion of the demyelinating lesion, and this was accompanied by aggravation of sensorimotor behavioral deficits. Therefore, our data reveal a function of HMGB1 as an autocrine trophic factor for OLs implicated in the preservation of white matter integrity in response to ischemic stress.

HMGB1 is ubiquitously expressed in almost all eukaryotic cells (27). In the brain, HMGB1 expression has been observed in neurons, astrocytes, microglial cells, and endothelial cells (28–30). Our study showed that HMGB1 is expressed in cultured OLs and OLs in the white matter in vivo. Only a few studies have reported HMGB1 expression in OLs (14, 31), but there is no report of cytoplasmic translocation or extracellular release of HMGB1 in OLs in response to cellular stress as demonstrated in our study. Our time-lapse imaging of OLs transfected with HMGB1–GFP and Western blot analysis of HMGB1 in the culture medium revealed that extracellular release of HMGB1 started to occur within an hour after ischemic insult. This is consistent with the finding that HMGB1 release occurs in the striatum as early as 30 min after middle cerebral artery occlusion (30). HMGB1 can be released passively from dying cells or secreted actively upon inflammatory stimuli without accompanying cell death (27). The HMGB1 release from OLs in our study is highly likely to be a passive process because it was accompanied by OGD-induced OL death. The relatively rapid occurrence of the HMGB1 release is also compatible with passive release because active secretion usually begins only several hours after proinflammatory stimulation (32). Damaged cells release various factors other than HMGB1 that can function as danger-associated molecular pattern (DAMP) proteins (33). Because we did not attempt to identify secreted proteins in CM in an unbiased manner, it is highly likely

that there may be factors other than HMGB1 with similar functions and future studies will be required to identify these factors.

HMGB1 released from damaged or dying cells stimulates innate immunity in neighboring cells (34, 35). The inflammatory reactions are thought to prevent initial damage that has caused cell death from spreading to adjacent tissue. It is possible that extracellularly released HMGB1 could be a signal to evoke innate immunity when it binds to TLRs expressed in microglial cells. However, our data showed that inhibition of HMGB1 by glycyrrhizin did not affect the extent of microglial activation in our white matter stroke model, suggesting that the presence of HMGB1 did not promote poststroke inflammation. Furthermore, CM obtained from cultured microglial cells treated with HMGB1 did not aggravate the OL death in response to OGD, whereas CM from LPS-treated microglial cells did. The distinct outcomes may derive from activation of different TLRs by the two ligands: LPS binds to TLR4 and HMGB1 to both TLR2 and TLR4 (36). LPS is one of the prototypical stimuli that drives M1 polarization and proinflammatory activity (37). Recent studies have shown that selective TLR2 activation leads to M2 polarization of microglial cells and provides neuroprotective and proregenerative effects (38, 39). Because HMGB1 released from dying OLs can bind to both TLR2 and TLR4, it may activate M2-like properties in microglial cells through TLR2 to counterbalance the cytotoxic effects of proinflammatory cytokines stimulated by TLR4. Thus, it is conceivable that the effects of HMGB1 release from dying neural cells on inflammation could be modulated by the differential expression of pattern recognition receptors in microglial cells (39).

In addition to their proinflammatory roles, recent studies have linked DAMPs to noninflammatory functions such as promoting cellular migration and proliferation, angiogenesis, and tissue repair (33, 40). In particular, HMGB1 was shown to contribute to spinal cord regeneration in animal models where spontaneous regeneration occurs (41, 42). Our data, showing that HMGB1 released from damaged OLs provides protective effects on OLs under ischemic stress, add a cellular trophic function to the list of the noninflammatory biological effects of HMGB1. HMGB1 involved in tissue repair or angiogenesis often stimulates cell types different from its origin. For example, HMGB1 released from grafted skin mobilizes bone marrow-derived epithelial progenitors to repair epidermal defects (43). In the brain, astrocyte-derived HMGB1 promotes proliferation of endothelial progenitor cells to contribute to neurovascular remodeling following stroke (44). In our study, the source and target cell types are the same and HMGB1 therefore provides an autocrine trophic signal for OLs. OLs use other autocrine signaling mechanisms. For example, developing OLs regulate their own survival and differentiation via the neuregulin–erbB receptor autocrine loop (45, 46), and galanin was identified as an autocrine trophic signal in cytokine-treated OLs and in the cuprizone-induced demyelination model (47). The HMBG1-mediated autocrine trophic signaling evidenced in our study may harnesses neighboring OLs with a sort of self-defense system against ischemic injuries to the white matter.

In our white matter stroke model with ET-1 injection, we observed cytoplasmic translocation of HMGB1. It is highly likely that HMGB1 was ultimately released extracellularly in response to ischemic stress induced by ET-1. Our finding that TLR2-dependent activation of ERK1/2 and CREB signaling following ET-1 injection was largely attenuated by glycyrrhizin suggests that extracellularly released HMGB1 binds to TLR2 as an endogenous ligand in vivo. Coinjection of glycyrrhizin resulted in a substantial expansion of the ET-1–induced demyelinating pathology, demonstrating that HMGB1 released by ischemic insult provides protective effects in myelinated white matter. The volume of the demyelinating lesion correlated with the degree of behavioral deficits, indicating that limiting the extent of demyelinating pathology is functionally meaningful. In addition to effects on OLs, HMGB1 may have beneficial effects on endothelial remodeling, another physiological process relevant to ischemia. A recent study showed that astrocytic HMGB1 in the periinfarct cortex stimulated endothelial progenitor cell proliferation and contributed to neurovascular remodeling in a focal cerebral ischemia (48). Furthermore, HMGB1 also enhances accumulation of endothelial progenitors in damaged white matter (44). Therefore, it is possible that OL-derived HMGB1 could promote endothelial cell remodeling in the vicinity of the lesion core.

In conclusion, HMGB1 is a stress-induced endogenous signal whose function is to maintain structural and functional integrity of the white matter under ischemic conditions. Manipulating this endogenous pathway may aid in developing new therapies for white matter stroke.

Materials and Methods

Primary OL and Microglial Cell Culture. Primary OL and microglial cell cultures were prepared from cortices of postnatal day 0 (P0) or P1 newborn wild-type and/or TLR2 (–/–) mice as previously described, with some modifications (49–51). The animal protocols were approved by Ajou University Institutional Animal Care and Use Committee. The cortices were dissociated into single cells and plated into a T25-cm^2 flask with DMEM supplemented with 10% FBS, 1% penicillin–streptomycin, and 1% GlutaMAX. Confluent mixed glial cultures were obtained after 9–10 d in vitro. Mixed glial cultures were shaken at 200 rpm at 37 °C for 1 h to remove microglial cells. Separated microglia were filtered through a nylon mesh to remove remnant astrocytes and cell clumps and maintained in DMEM with 10% FBS. A second cycle of shaking was performed at 250 rpm at 37 °C for 18 h to remove OLs from the monolayer of astrocytes. Cell suspensions were plated onto a bacterial grade Petri dish for 1 h to separate OLs from remaining astrocytes. Purified OLs were plated onto a poly-D-lysine–coated 12-well (1.5×10^5 cells per well) or 96-well (1.5×10^4 cells per well) plates or 9-mm coverslips (1.0×10^4 cells per coverslip) in serum-free differentiation media consisting of high glucose DMEM, 2% B27, 1% GlutaMAX, 0.1% BSA, transferrin (100 μg/mL), putrescine (20 μg/mL), progesterone (12.8 ng/mL), selenium (10.4 ng/mL), insulin (50 μg/mL), and thyroxine (0.8 μg/mL).

In Vitro OGD Insult and Collection of CM. For OGD insult, OLs cultured for 24 h in serum-free differentiation medium were washed with PBS and transferred to an anaerobic chamber (Forma Scientific). The culture medium was replaced with the glucose-free differentiation medium that had been saturated with N_2 gas for 1 h. The cultured OLs were exposed to OGD for 2 h and then transferred to a normoxic chamber. The culture medium was replaced with fresh medium containing glucose and various pharmacological reagents, including recombinant HMGB1 (Sigma) in sterile endotoxin-free PBS or glycyrrhizin (Sigma) in distilled water with pH adjusted to 7.4. In experiments to examine effects of various CMs on OL death, the culture medium was replaced with CM collected from cultured OLs or microglial cells. Microglial CM (MCM) was collected from primary microglial cultures for 72 h after the 3-h incubation with LPS (100 ng/mL) or HMGB1 (1 ng/mL). To collect CM from cultured OLs exposed to OGD, OLs were incubated for 6 h after OGD completion because we found consistent HMGB1 immunoreactivity in the media at this time point (Fig. 1*A*). Collected CMs were centrifuged at $100 \times g$ for 2 min and passed through a 0.2-μm filter (BD Biosciences) to remove any remnant cellular debris before application to cultured OLs for lactate dehydrogenase (LDH) assay. Immunodepletion of CM was performed as previously described with a slight modification (52). Briefly, collected CM was incubated with anti-HMGB1 antibody (Abcam, ab18256; 4 μg/mL) overnight at 4 °C. The CM–antibody complexes were further incubated with 30 μL of protein A/G-agarose beads (Pierce) for 2 h. After centrifugation, the supernatant was recollected as HMGB1-depleted CM (ΔCM) and the beads were thoroughly washed with washing buffer and heated in 2× sample buffer for immunoblotting to confirm the presence of HMGB1 in the fraction containing the agarose beads.

LDH Assays. For quantification of OGD-induced OL death, LDH assays were performed 24 h after the onset of OGD (22 h after the end of the 2-h OGD session) using an assay kit (Takara Bio). The LDH level corresponding to complete cell death was determined in sister cultures exposed to 1.5% Triton X-100 for 24 h [complete death (CD)]. Baseline LDH levels were determined in a condition of media alone without any cells [baseline (BL)]. The percentage of cell death in each experimental condition was calculated using the following formula: % of OL death = 100 × (experimental value − BL)/(CD − BL).

Transfection of Primary OLs. For transfecting the HMGB1–GFP plasmid (Origene) or HMGB1 siRNA (Santa Cruz, sc37983) into cultured primary OLs, we

used the Amaxa Nucleofactor electroporation system (Lonza). Briefly, purified OLs were grown in neurobasal medium supplemented with 2% B27 and PDGF (10 ng/mL) for several days, allowing continuous proliferation. After confluence was reached, OLs were detached from the cell culture plates, transferred to a conical tube, and centrifuged at 90 × *g* for 10 min. Pelleted OLs were resuspended with Nucleofactor solution and HMGB1–GFP plasmid or HMGB1 siRNA and transferred to an electroporation cuvette. Finally, resuspended OLs in a cuvette were electroporated using the Nucleofactor II machine (program no. A-033). OL media were replaced immediately after electroporation. OLs were plated onto culture dishes for immunoblotting or LDH assays or onto glass-bottom culture dishes for time-lapse live cell imaging.

Fluorescence Time-Lapse Imaging. Cultured OLs transfected with HMGB1–GFP plasmid were plated on a culture dish with a glass bottom and incubated within a chamber attached to the fluorescence time-lapse microscope (Nikon Eclipse) for 24 h. The live imaging system is not equipped with a cell culture chamber enabling hypoxia. Therefore, we induced chemical hypoxia using $CoCl_2$, which is a frequently used hypoxia-mimetic reagent (53). To mimic OGD insult, the bathing medium was replaced with glucose-free medium containing $CoCl_2$ (200 μM; Sigma). Hoechst 33342 dye was added into the bathing media to stain nuclei 30 min before $CoCl_2$ application. GFP^+ cells were identified under the microscope and the time-lapse images were captured immediately after the $CoCl_2$ application for 4 h at 5-min intervals.

Animals and Surgical Procedures. Nine- to 10-week-old adult male C57BL/6 mice, weighing 25–28 g, were used. The animal protocols were approved by Ajou University Institutional Animal Care and Use Committee. Mice were anesthetized with i.p. injection of 4% chloral hydrate (400 mg/kg) injection. After anesthetization, the head was anchored to a stereotaxic frame and a craniotomy was made with a drill. Stereotaxic injection of drugs was performed as described previously (9). The target coordinates were as follows: −1.0 posterior from the bregma, −2.8 mm lateral from the midline, and −4.3 mm ventral from the skull surface. The needle was angled away from the injection site at 20° from the midline to avoid potential damage to the hippocampal structures. One microliter of ET-1 (1 mg/mL; Bachem) with sterile PBS or glycyrrhizin (240 μM) was injected for 5 min, the needle was left in place for 10 min, and then it was slowly removed from the brain.

Behavioral Analysis. The corner test assesses sensory and motor asymmetries after ischemic injuries (17–19). The corner apparatus consists of two wooden boards (30 cm × 20 cm × 1 cm) that are attached to each other at a 30° angle. There is a small slit-like opening where the two boards join (corner) to encourage animals to enter into the corner end of the apparatus. Mice are allowed to walk into the corner after placement at the midline in the open end. As mice walk into the corner, boards at each side stimulate bilateral vibrissae, and then the animals rear up on their hindlimbs and turn back to face the open end. We considered a trial as complete only when rearing up preceded turning back to the open end (17). The direction of rearing up and turning back was recorded for a total of 10 trials per animal. The percentage of ipsilesional turns was calculated as an indicator of deficit severity because ischemic mice showed a preference for turning toward the nonimpaired side (ipsilesional side). The tests were performed once before ET-1 injection to record the baseline percentage value as a control and every day after ET-1 injection until 7 d postinjection.

The pole test is used to examine motor dysfunction after ischemic injuries (19, 20). The pole apparatus is made by placing a 50-cm-long pole with a 10-cm-diameter flat top inside a home cage. The pole surface is wrapped in adhesive tape to provide traction. Mice are positioned head upward at the top of pole. There are two outcome parameters in the pole test. One is time to turn, the duration from starting with the head positioned upward at the top of the pole to turning the head downward completely. The other parameter is time to floor, the time taken to descend the pole apparatus and reach the home cage floor. Mice were tested five times per day and the average of the five trials was obtained as the data for each day. If mice dropped to the floor before completing the descent, a retrial was done. Mice were trained and the baseline values were obtained before ET-1 injection and then tested every day after ET-1 injection until 7 d postinjection.

Statistical Analysis. All numerical values and error bars in the quantification graphs are expressed as mean ± SEM. Statistical comparison of mean values was performed using Student's *t* test for two independent groups or one-way ANOVA followed by Tukey's post hoc test for three and more independent groups. For statistical comparison of behavioral tests performed at multiple time points, repeated-measures two-way ANOVA was performed with Bonferroni's post hoc test. Pearson's correlation analysis was performed to examine the relationship between the behavioral outcomes and the volumes of the demyelinating lesions. All quantification graphs were generated using GraphPad Prism software version 5.0 (GraphPad Software). Additional materials and methods are available in *SI Materials and Methods*.

ACKNOWLEDGMENTS. This study was supported by the Korean Health Technology Research and Development Project, Ministry of Health and Welfare, Republic of Korea (Grant HI13C1850) and by the National Research Foundation of Korea (Grant NRF-2012R1A5A2048183).

1. Walhovd KB, Johansen-Berg H, Káradóttir RT (2014) Unraveling the secrets of white matter: Bridging the gap between cellular, animal and human imaging studies. *Neuroscience* 276:2–13.
2. Karadottir RT, Walhovd KB (2014) The CNS white matter. *Neuroscience* 276:1.
3. McKenzie IA, et al. (2014) Motor skill learning requires active central myelination. *Science* 346:318–322.
4. Richardson WD, Young KM, Tripathi RB, McKenzie I (2011) NG2-glia as multipotent neural stem cells: fact or fantasy? *Neuron* 70:661–673.
5. Simpson JE, et al.; MRC Cognitive Function and Ageing Neuropathology Study Group (2007) White matter lesions in an unselected cohort of the elderly: Astrocytic, microglial and oligodendrocyte precursor cell responses. *Neuropathol Appl Neurobiol* 33:410–419.
6. Young VG, Halliday GM, Kril JJ (2008) Neuropathologic correlates of white matter hyperintensities. *Neurology* 71:804–811.
7. Decavel P, Vuillier F, Moulin T (2012) Lenticulostriate infarction. *Front Neurol Neurosci* 30:115–119.
8. Román GC, Erkinjuntti T, Wallin A, Pantoni L, Chui HC (2002) Subcortical ischaemic vascular dementia. *Lancet Neurol* 1:426–436.
9. Choi JY, et al. (2014) Role of toll-like receptor 2 in ischemic demyelination and oligodendrocyte death. *Neurobiol Aging* 35:1643–1653.
10. Vabulas RM, et al. (2001) Endocytosed HSP60s use toll-like receptor 2 (TLR2) and TLR4 to activate the toll/interleukin-1 receptor signaling pathway in innate immune cells. *J Biol Chem* 276:31332–31339.
11. Vabulas RM, et al. (2002) HSP70 as endogenous stimulus of the Toll/interleukin-1 receptor signal pathway. *J Biol Chem* 277:15107–15112.
12. Park JS, et al. (2004) Involvement of toll-like receptors 2 and 4 in cellular activation by high mobility group box 1 protein. *J Biol Chem* 279:7370–7377.
13. Park KI, et al. (2006) Neural stem cells may be uniquely suited for combined gene therapy and cell replacement: Evidence from engraftment of Neurotrophin-3-expressing stem cells in hypoxic-ischemic brain injury. *Exp Neurol* 199:179–190.
14. Kim JB, Lim CM, Yu YM, Lee JK (2008) Induction and subcellular localization of high-mobility group box-1 (HMGB1) in the postischemic rat brain. *J Neurosci Res* 86:1125–1131.
15. Mollica L, et al. (2007) Glycyrrhizin binds to high-mobility group box 1 protein and inhibits its cytokine activities. *Chem Biol* 14:431–441.
16. Akira S, Takeda K (2004) Toll-like receptor signalling. *Nat Rev Immunol* 4:499–511.
17. Zhang L, et al. (2002) A test for detecting long-term sensorimotor dysfunction in the mouse after focal cerebral ischemia. *J Neurosci Methods* 117:207–214.
18. Schaar KL, Brenneman MM, Savitz SI (2010) Functional assessments in the rodent stroke model. *Exp Transl Stroke Med* 2:13.
19. Park SY, et al. (2014) A method for generating a mouse model of stroke: Evaluation of parameters for blood flow, behavior, and survival [corrected]. *Exp Neurobiol* 23:104–114.
20. Bouët V, et al. (2007) Sensorimotor and cognitive deficits after transient middle cerebral artery occlusion in the mouse. *Exp Neurol* 203:555–567.
21. Frank MG, et al. (2016) The danger-associated molecular pattern HMGB1 mediates the neuroinflammatory effects of methamphetamine. *Brain Behav Immun* 51:99–108.
22. Fonken LK, et al. (2016) The alarmin HMGB1 mediates age-induced neuroinflammatory priming. *J Neurosci* 36:7946–7956.
23. Nakazawa T, et al. (2006) Tumor necrosis factor-alpha mediates oligodendrocyte death and delayed retinal ganglion cell loss in a mouse model of glaucoma. *J Neurosci* 26:12633–12641.
24. Takahashi JL, Giuliani F, Power C, Imai Y, Yong VW (2003) Interleukin-1beta promotes oligodendrocyte death through glutamate excitotoxicity. *Ann Neurol* 53:588–595.
25. Schönrock LM, Gawlowski G, Brück W (2000) Interleukin-6 expression in human multiple sclerosis lesions. *Neurosci Lett* 294:45–48.
26. Cui QL, Almazan G (2007) IGF-I-induced oligodendrocyte progenitor proliferation requires PI3K/Akt, MEK/ERK, and Src-like tyrosine kinases. *J Neurochem* 100:1480–1493.
27. Yang H, Wang H, Czura CJ, Tracey KJ (2005) The cytokine activity of HMGB1. *J Leukoc Biol* 78:1–8.
28. Sun Y, et al. (2015) HMGB1 expression patterns during the progression of experimental autoimmune encephalomyelitis. *J Neuroimmunol* 280:29–35.
29. Faraco G, et al. (2007) High mobility group box 1 protein is released by neural cells upon different stresses and worsens ischemic neurodegeneration in vitro and in vivo. *J Neurochem* 103:590–603.
30. Qiu J, et al. (2008) Early release of HMGB-1 from neurons after the onset of brain ischemia. *J Cereb Blood Flow Metab* 28:927–938.
31. Daston MM, Ratner N (1994) Amphoterin (P30, HMG-1) and RIP are early markers of oligodendrocytes in the developing rat spinal cord. *J Neurocytol* 23:323–332.
32. Wang H, et al. (1999) HMG-1 as a late mediator of endotoxin lethality in mice. *Science* 285:248–251.

33. Vénéreau E, Ceriotti C, Bianchi ME (2015) DAMPs from cell death to new life. *Front Immunol* 6:422.
34. Chan JK, et al. (2012) Alarmins: Awaiting a clinical response. *J Clin Invest* 122: 2711–2719.
35. Scaffidi P, Misteli T, Bianchi ME (2002) Release of chromatin protein HMGB1 by necrotic cells triggers inflammation. *Nature* 418:191–195.
36. Yu L, Wang L, Chen S (2010) Endogenous toll-like receptor ligands and their biological significance. *J Cell Mol Med* 14:2592–2603.
37. Martinez FO, Sica A, Mantovani A, Locati M (2008) Macrophage activation and polarization. *Front Biosci* 13:453–461.
38. Stirling DP, et al. (2014) Toll-like receptor 2-mediated alternative activation of microglia is protective after spinal cord injury. *Brain* 137:707–723.
39. Gensel JC, et al. (2015) Toll-like receptors and dectin-1, a C-type lectin receptor, trigger divergent functions in CNS macrophages. *J Neurosci* 35:9966–9976.
40. Pandolfi F, Altamura S, Frosali S, Conti P (2016) Key role of DAMP in inflammation, cancer, and tissue repair. *Clin Ther* 38:1017–1028.
41. Dong Y, et al. (2013) HMGB1 protein does not mediate the inflammatory response in spontaneous spinal cord regeneration: A hint for CNS regeneration. *J Biol Chem* 288: 18204–18218.
42. Fang P, et al. (2014) HMGB1 contributes to regeneration after spinal cord injury in adult zebrafish. *Mol Neurobiol* 49:472–483.
43. Tamai K, et al. (2011) PDGFRalpha-positive cells in bone marrow are mobilized by high mobility group box 1 (HMGB1) to regenerate injured epithelia. *Proc Natl Acad Sci USA* 108:6609–6614.
44. Hayakawa K, et al. (2013) High-mobility group box 1 from reactive astrocytes enhances the accumulation of endothelial progenitor cells in damaged white matter. *J Neurochem* 125:273–280.
45. Raabe TD, Clive DR, Wen D, DeVries GH (1997) Neonatal oligodendrocytes contain and secrete neuregulins in vitro. *J Neurochem* 69:1859–1863.
46. Deadwyler GD, Pouly S, Antel JP, Devries GH (2000) Neuregulins and erbB receptor expression in adult human oligodendrocytes. *Glia* 32:304–312.
47. Gresle MM, et al. (2015) Galanin is an autocrine myelin and oligodendrocyte trophic signal induced by leukemia inhibitory factor. *Glia* 63:1005–1020.
48. Hayakawa K, Pham LD, Katusic ZS, Arai K, Lo EH (2012) Astrocytic high-mobility group box 1 promotes endothelial progenitor cell-mediated neurovascular remodeling during stroke recovery. *Proc Natl Acad Sci USA* 109:7505–7510.
49. O'Meara RW, Ryan SD, Colognato H, Kothary R (2011) Derivation of enriched oligodendrocyte cultures and oligodendrocyte/neuron myelinating co-cultures from postnatal murine tissues. *J Vis Exp* :e3324.
50. Giulian D, Baker TJ (1986) Characterization of ameboid microglia isolated from developing mammalian brain. *J Neurosci* 6:2163–2178.
51. Kim JH, Min KJ, Seol W, Jou I, Joe EH (2010) Astrocytes in injury states rapidly produce anti-inflammatory factors and attenuate microglial inflammatory responses. *J Neurochem* 115:1161–1171.
52. Lu J, et al. (2013) Endothelial cells promote the colorectal cancer stem cell phenotype through a soluble form of Jagged-1. *Cancer Cell* 23:171–185.
53. Triantafyllou A, et al. (2006) Cobalt induces hypoxia-inducible factor-1alpha (HIF-1alpha) in HeLa cells by an iron-independent, but ROS-, PI-3K- and MAPK-dependent mechanism. *Free Radic Res* 40:847–856.
54. Donnelly DJ, Gensel JC, Ankeny DP, van Rooijen N, Popovich PG (2009) An efficient and reproducible method for quantifying macrophages in different experimental models of central nervous system pathology. *J Neurosci Methods* 181:36–44.